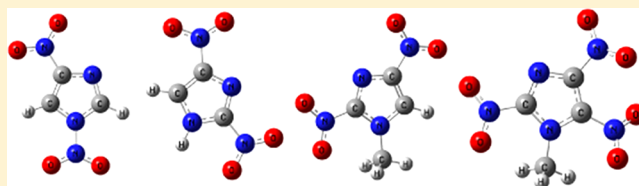


On the Decomposition Mechanisms of New Imidazole-Based Energetic Materials

Zijun Yu and Elliot R. Bernstein*

Department of Chemistry, Colorado State University, Fort Collins, Colorado 80523-1872, United States

ABSTRACT: New imidazole-based energetic molecules (1,4-dinitroimidazole, 2,4-dinitroimidazole, 1-methyl-2,4-dinitroimidazole, and 1-methyl-2,4,5-trinitroimidazole) are studied both experimentally and theoretically. The NO molecule is observed as a main decomposition product from the above nitroimidazole energetic molecules excited at three UV wavelengths (226, 236, and 248 nm). Resolved rotational spectra related to three vibronic bands (0–0), (0–1), and (0–2) of the NO ($A^2\Sigma^+ \leftarrow X^2\Pi$) electronic transition have been obtained. A unique excitation wavelength independent dissociation channel is characterized for these four nitroimidazole energetic molecules: this pathway generates the NO product with a rotationally cold (10–60 K) and vibrationally hot (1300–1600 K) internal energy distribution. The predicted reaction mechanism for the nitroimidazole energetic molecule decomposition subsequent to electronic excitation is the following: electronically excited nitroimidazole energetic molecules descend to their ground electronic states through a series of conical intersections, dissociate on their ground electronic states subsequent to a nitro–nitrite isomerization, and produce NO molecules. Different from PETN, HMX, and RDX, the thermal dissociation process (ground electronic state decomposition from the Franck–Condon equilibrium point) of multinitroimidazoles is predicted to be a competition between NO₂ elimination and nitro–nitrite isomerization followed by NO elimination for all multinitroimidazoles except 1,4-dinitroimidazole. In this latter instance, N–NO₂ homolysis becomes the dominant decomposition channel on the ground electronic state, as found for HMX and RDX. Comparison of the stability of nitro-containing energetic materials with R–NO₂ (R = C, N, O) moieties is also discussed. Energetic materials with C–NO₂ are usually more thermally stable and impact/shock insensitive than are other energetic materials with N–NO₂ and O–NO₂ moieties. The imidazole aromatic ring also plays an important role in improving the stability of these energetic materials. Thus, multinitroimidazoles energetic materials can be of significant potential for both civilian and military applications.



I. INTRODUCTION

Energetic materials, including explosives and propellants that are useful for a variety of military purposes and industrial applications, have been studied for decades.^{1–11} In order to meet future civilian and military safety and environmental requirements, research efforts have been undertaken to develop new energetic materials.^{12–14} Among these new molecules, imidazole-based energetic species have drawn particular attention due to their high heats of formation, favorable detonation performance, good thermal stabilities, and impact and shock insensitivity.

Previous studies of these compounds have focused on the synthesis of novel imidazole-based derivatives, some of which have significant biological activity,¹⁵ or on the development of new synthetic pathways.¹⁶ A few studies have concentrated on the physical and chemical properties of imidazole-based energetic materials.^{17–23}

Our previous studies of this general system have already reported the unimolecular, isolated molecule, decomposition of mononitroimidazoles (model systems), which are chemically and physically similar to the dinitroimidazole energetic materials but are not themselves energetic.²⁴ In this case, the NO radical is detected as the initial product of the decomposition of electronically excited mononitroimidazoles. Mononitroimidazoles,²⁴ which serve as model systems for

aromatic imidazole energetic materials, dissociate from electronic excited states and give rotationally cold and vibrationally warm distributions of the NO product. On the other hand, DMNA (dimethylnitramine),²⁵ which serves as a model molecule for the nonaromatic energetic nitramines RDX (hexahydro-1,3,5-trinitro-1,3,5-triazine), HMX (octahydro-1,3,5,7-tetranitro-1,3,5,7-tetrazocine), CL20 (2,4,6,8,10,12-hexanitro-2,4,6,8,10,12-hexaazaisowurtzitane), etc., dissociates from electronic excited states and gives rotationally hot and vibrationally cold distributions of the NO product. Again unlike DMNA, the mononitroimidazoles have ground state barriers for NO₂ elimination and nitro–nitrite isomerization that are comparable to one another, suggesting that these two channels are competitive for solely ground state decomposition from the equilibrium S₀ structure. Given these model system differences between aromatic (mononitroimidazoles) and nonaromatic (DMNA) model species, the comparison of energy release from aromatic (imidazole based) and nonaromatic (RDX, HMX, PETN (pentaerythritoltetranitrate), etc.) energetic systems should prove quite interesting and important for the

Received: December 19, 2012

Revised: February 4, 2013

Published: February 7, 2013



fundamental understanding of the conversion of chemical energy to mechanical energy.

Investigations of the gas phase, isolated molecule decomposition of these nitroimidazoles following electronic excitation will yield an improved understanding of the initial decomposition mechanisms and dynamics for imidazole-based energetic materials, as the decomposition mechanism must first be of a molecular nature in an organic crystal. For discussion about, and references to, generation of excited electronic states through mechanical pressure on solids (triboluminescence), see ref 26.

In this report, we focus on understanding the decomposition mechanism and dynamics of imidazole-based energetic molecules (1,4-dinitroimidazole, 2,4-dinitroimidazole, 1-methyl-2,4-dinitroimidazole, and 1-methyl-2,4,5-trinitroimidazole, structures shown in Figure 1) based on experiments and ab

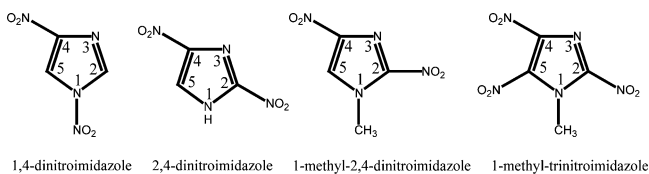


Figure 1. Molecular structures of four nitroimidazole energetic molecules.

initio quantum calculations. Nanosecond energy resolved spectroscopy is employed to investigate the electronic excited state decomposition mechanisms and dynamics of the above isolated gas phase multinitroimidazole energetic molecules. Several detailed insights into the unimolecular decomposition behavior of these multinitroimidazole energetic molecules from their electronic excited states and ground state will be discussed. Different reaction channels, such as NO_2 elimination, nitro–nitrite isomerization channels, and HONO elimination, will be discussed for ground electronic state decomposition from the Franck–Condon equilibrium point. Conical intersections for 1,4-dinitroimidazole and 2,4-dinitroimidazole are explored by the Complete Active Space Multiconfiguration Self Consistent Field (CASSCF) methods to analyze the decomposition mechanism for electronically excited multinitroimidazole energetic molecules. Comparison between energetic materials with $\text{R}-\text{NO}_2$ ($\text{R} = \text{C}, \text{N}, \text{O}$) moieties will be considered in order to aid in the design of new energetic materials with better stability and impact/shock insensitivity for explosive applications.

II. EXPERIMENTAL PROCEDURES

The experimental setup consists of nanosecond (ns) laser systems, a supersonic jet expansion pulsed nozzle, and a time-of-flight mass spectrometer chamber, described in detail elsewhere.^{27,28} Briefly, for the ns laser experiments, a single pump–probe laser beam is employed to excite the energetic molecule, and probe and ionize the NO product. The laser wavelength is separately set to 226, 236, 248 nm to access the $\text{A } ^2\Sigma^+(v'=0) \leftarrow \text{X } ^2\Pi (v''=0,1,2)$ transition. The NO product is detected by a one-color (1 + 1) resonance-enhanced, two-photon ionization (R2PI) scheme ($\text{A } ^2\Sigma^+(v'=0) \leftarrow \text{X } ^2\Pi (v''=0,1,2)$ transition by absorption of the first photon and then ionization of the NO molecule by absorption of the second photon) through time-of-flight mass spectrometry (TOFMS). Samples (1,4-dinitroimidazole, 2,4-dinitroimidazole, 1-methyl-

2,4-dinitroimidazole, and 1-methyl-2,4,5-trinitroimidazole) were supplied by Dr. Rao Surapaneni and Mr. Reddy Damavarapu (ARL, Picatinny Arsenal, N. J.). The isolated gas phase 1,4-dinitroimidazole and 2,4-dinitroimidazole molecules are produced through a combination of matrix assisted laser desorption (MALD) and supersonic jet expansion. The nozzle employed for the sample beam generation is constructed from a Jordan Co. pulsed valve and a laser desorption attachment.²⁷ Sample drums for matrix desorption are prepared by wrapping a piece of porous filter paper around a clean aluminum drum. A solution of equimolar amounts of sample and matrix (R6G dye) in acetone is uniformly sprayed on the sample drum. An air atomizing spray nozzle (Spraying System Co.) with siphon pressure of 10 psi is used to deposit ablation samples on the filter paper surface. During the spraying, the drum with attached filter paper is rotated and heated with a halogen lamp to make sure that the sample coating is homogeneous and dry. The dried sample drum is then placed in the laser ablation head/nozzle assembly and put into a vacuum chamber. To maintain a fresh sample area for each laser ablation shot, a single motor is used to rotate and translate the sample drum simultaneously. Due to their high vapor pressure, the isolated gas phase 1-methyl-2,4-dinitroimidazole and 1-methyl-2,4,5-trinitroimidazole cannot be generated by the MALD method; these samples are vaporized by heating the nozzle. The imidazole-based energetic molecules, desorbed from the drum by laser ablation at 532 nm or produced by heating, are entrained in the flow of helium gas through a 2×60 mm channel in the ablation head, and are expanded into the vacuum chamber.

The experiment is run at a repetition rate of 10 Hz. The timing sequence for the pulsed nozzle, ablation laser, and ionization laser is controlled by a time delay generator (SRS DG535). The molecular beam is perpendicularly crossed by a UV laser beam that is focused to a spot size of about 0.5 mm at the ionization region of a time-of-flight mass spectrometer. A background pressure of 2×10^{-6} Torr is maintained in the vacuum chamber during the experiment. Ion signals are detected by a microchannel plate detector. Signals are recorded and processed on a personal computer, using a boxcar averager (SRS SR 250) and an analog-to-digital conversion card (Analog Devices RTI-800).

III. COMPUTATIONAL METHODS

All calculations are carried out within the Gaussian 09 program.²⁹ To choose a proper calculation method for multinitroimidazole molecules, MP2 and density functional theory (DFT) methods are applied to calculate the $\text{R}-\text{NO}_2$ bond dissociation energy (including zero-point energies correction), in which R denotes the remainder of the nitroaromatic molecule. Table 1 lists the bond dissociation energy for each nitroaromatic molecule with the corresponding experimental result for the system. Bond dissociation energies predicated by DFT method are in good agreement with the experimental results, while the MP2 results are not. Thus the DFT method, especially B3P86 and B3LYP, which have been widely applied to investigate energetic compounds,^{30–35} was used to calculate the NO_2 elimination, nitro–nitrite isomerization, and HONO elimination reaction channels on the ground potential energy surface for nitroimidazole energetic compounds.

TD-DFT³⁷ methods using the LC- ω PBE³⁸ and LC-BLYP³⁹ density functional with aug-cc-pVDZ basis set are applied to

Table 1. Computed Bond Dissociation Energies (kcal/mol) at 298 K on Their Ground State Potential Energy Surfaces from the Franck–Condon Equilibrium Geometry for Various Nitroaromatics by MP2 and DFT Computational Methods^a

| compd ^b | MP2/6 -311G(d,p) | B3P86/6 -311G(d,p) | exptl ^c |
|----------------------------------------------------------------------------------------|---------------------|-----------------------|--------------------|
| C ₆ H ₅ -NO ₂ | 97.8 | 70.7 | 70.7 ± 1 |
| 3-NO ₂ -C ₆ H ₄ -1-NO ₂ | 96.6 | 68.2 | 66.5 |
| 4-NO ₂ -C ₆ H ₄ -1-NO ₂ | 97.0 | 68.1 | 67.0 |
| 2-CH ₃ -C ₆ H ₄ -1-NO ₂ | 96.8 | 68.0 | 70.2 ± 2.5 |
| 4-CH ₃ -C ₆ H ₄ -1-NO ₂ | 99.0 | 71.8 | 71.4 ± 2.3 |
| 3,5-(NO ₂) ₂ -C ₆ H ₃ -1-NO ₂ | 95.5 | 66.1 | 66.0 |
| 2-CH ₃ -4-NO ₂ -C ₆ H ₃ -1-NO ₂ | 96.1 | 65.5 | 70.6 ± 2 |
| furan-2-NO ₂ | 86.6 | 74.0 | 70.4 |

^aZero-point energies are taken into account. ^bThe boldface emphasizes the dissociated nitro group. ^cThe data are from ref 36.

calculate the vertical excited energies for multinitroimidazoles. The geometry optimization on the ground state potential energy surface for nitroimidazoles is executed at the CASSCF(16, 12)/6-31G(d) level of theory.⁴⁰ Calculations with a large active space (16, 12) are too expensive for exploration of the potential energy surfaces of electronically excited states, especially requiring analytical second derivative analysis. Therefore, a smaller active space (8, 6) is used to perform the CASSCF calculations. The orbitals chosen for the small active space, which are illustrated in Figure 2, are bonding π_1

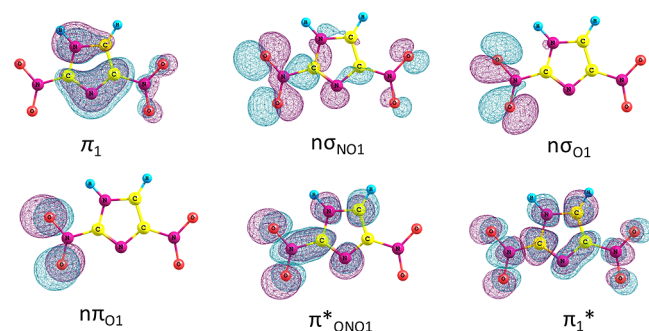


Figure 2. Orbitals used in the active space (8, 6) for CASSCF calculations for 2,4-dinitroimidazole are shown as an example.

and antibonding π_1^* orbitals of the five-member ring, NO nonbonding orbital $n\sigma_{NO1}$, π -nonbonding orbital $n\pi_{O1}$, π -nonbonding orbital $n\pi_{O1}$, and the delocalized ONO π -antibonding orbital π_{ONO1}^* . Since the chosen NO₂ orbitals are located only on one NO₂ group, the small active space cannot accurately represent the potential energy surface of the higher excited states: for these states the orbitals from two NO₂ groups and the five-member ring are coupled and interact with each other for the representation of the high excited states. Therefore, only transition states for NO elimination after the nitro–nitrite isomerization and the conical intersections between the ground state and first excited state are searched at the CASSCF(8, 6)/6-31G(d) level. Geometries of the conical intersections are optimized with state averaging over the S₀ and S₁ states with equal weights. Transition state structures are characterized by analytical frequency calculations. No symmetry restrictions are applied during the calculations.

IV. EXPERIMENTAL RESULTS

Four multinitroimidazoles (1,4-dinitroimidazole, 2,4-dinitroimidazole, 1-methyl-2,4-dinitroimidazole, and 1-methyl-2,4,5-trinitroimidazole) have been studied at three excitation wavelengths (226, 236, and 248 nm). The parent molecules are excited to an upper vibronic state by absorption of a single UV photon. They decompose into products through specific decomposition pathways. The NO product channel has been detected here as the major decomposition pathway of these multinitroimidazoles. (1 + 1) R2PI spectra of the three vibronic transitions, A $^2\Sigma^+(v'=0) \leftarrow X \ ^2\Pi (v''=0,1,2)$, of the NO product generated by the decomposition of the electronically excited energetic molecules (1,4-dinitroimidazole, 2,4-dinitroimidazole, 1-methyl-2,4-dinitroimidazole, and 1-methyl-2,4,5-trinitroimidazole) are shown in Figures 3–6. The most intense

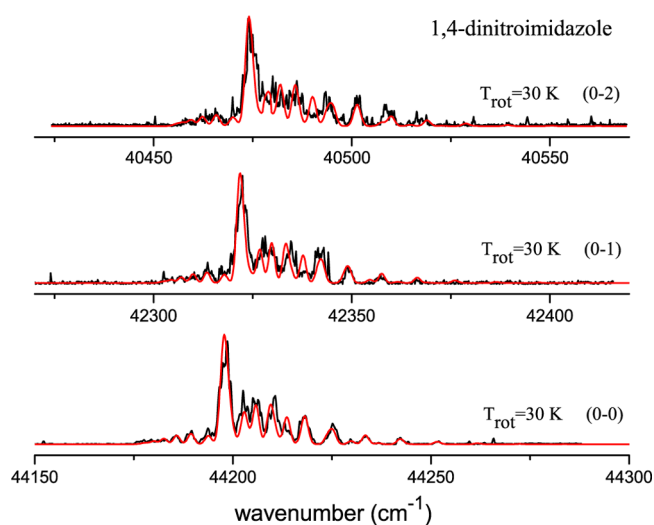


Figure 3. One color (1 + 1) R2PI spectra of the vibronic transitions A $^2\Sigma^+(v'=0) \leftarrow X \ ^2\Pi (v''=0,1,2)$ of NO products from the decomposition of electronically excited 1,4-dinitroimidazole. Rotational temperature simulations (red) with a Boltzmann population distribution show that these three observed vibrational levels of NO products have cold rotational temperatures of ~ 30 K. The vibrational temperature of NO products from 1,4-dinitroimidazole is estimated to be ~ 1600 K.

feature in each spectrum of NO can be assigned as the (Q_1+P_{12}) band head of each vibronic band, and the less intense features within each spectrum are due to other rovibronic transitions.^{41,42} Spectral simulations (red lines in Figures 3–6) based on Boltzmann population distributions for these vibronic transitions produce similar rotational temperatures of 10–60 K. The vibrational temperature of the NO product from these multinitroimidazoles can also be obtained by simulating the relative intensities among the observed vibronic bands, using a Boltzmann population distribution analysis and the Franck–Condon factors. By comparing the experimental data with simulations at different vibrational temperatures, the vibrational temperature of the NO product is about 1600, 1650, 1300, and 1350 K for 1,4-dinitroimidazole, 2,4-dinitroimidazole, 1-methyl-2,4-dinitroimidazole, and 1-methyl-2,4,5-trinitroimidazole, respectively. They all generate rotationally cold and vibrationally hot distributions of the NO product, as do all energetic molecules we have studied previously.^{43,44}

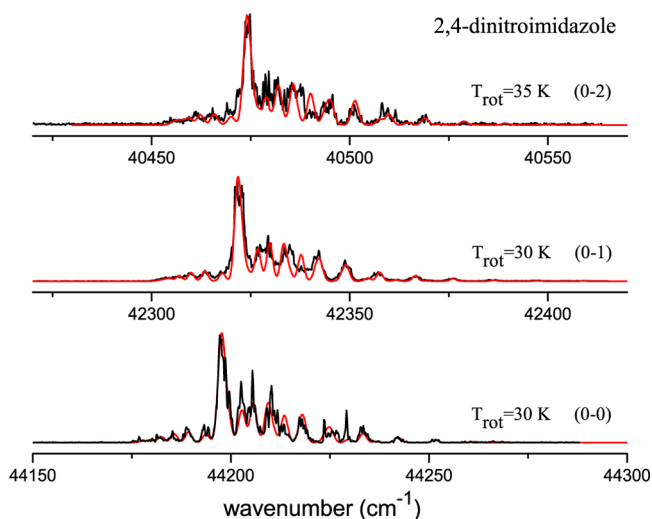


Figure 4. One color (1 + 1) R2PI spectra of the vibronic transitions $A^2\Sigma^+(v'=0) \leftarrow X^2\Pi(v''=0,1,2)$ of NO products from the decomposition of electronically excited 2,4-dinitroimidazole. Rotational temperature simulations (red) with a Boltzmann population distribution show that these three observed vibrational levels of NO products have cold rotational temperatures of 30–35 K. The vibrational temperature of NO products from 2,4-dinitroimidazole is estimated to be ~ 1650 K.

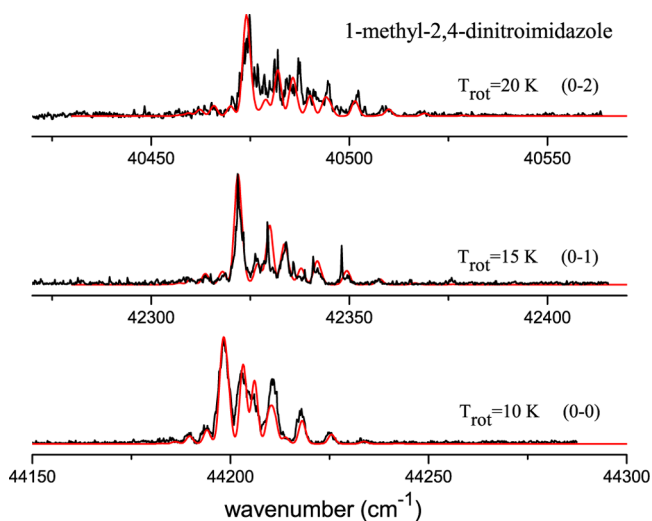


Figure 5. One color (1 + 1) R2PI spectra of the vibronic transitions $A^2\Sigma^+(v'=0) \leftarrow X^2\Pi(v''=0,1,2)$ of NO products from the decomposition of electronically excited 1-methyl-2,4-dinitroimidazole. Rotational temperature simulations (red) with a Boltzmann population distribution show that these three observed vibrational levels of NO products have cold rotational temperatures of 10–20 K. The vibrational temperature of NO products from 1-methyl-2,4-dinitroimidazole is estimated to be ~ 1300 K.

V. THEORETICAL RESULTS

A. Electronic Ground State Decomposition from the Franck–Condon Equilibrium Point. Three dissociation channels, NO_2 elimination, nitro–nitrite isomerization followed by NO elimination, and HONO elimination, could play important roles in the decomposition of nitroimidazoles on the electronic ground state surface. Theoretical exploration of these three reaction channels is considered below in order to

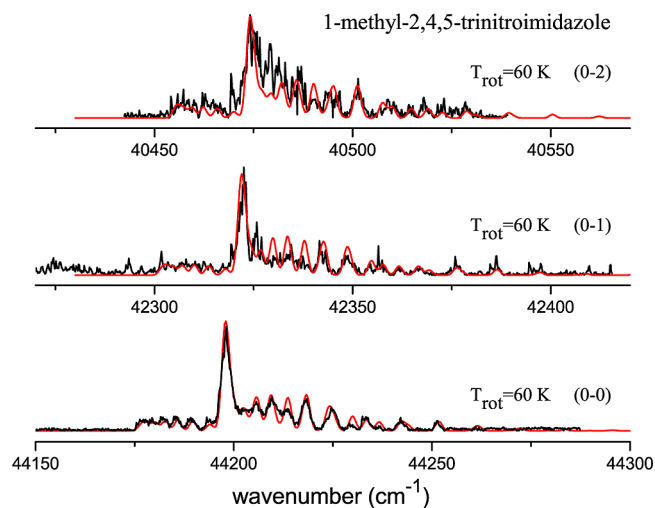


Figure 6. One color (1 + 1) R2PI spectra of the vibronic transitions $A^2\Sigma^+(v'=0) \leftarrow X^2\Pi(v''=0,1,2)$ of NO products from the decomposition of electronically excited 1-methyl-2,4,5-dinitroimidazole. Rotational temperature simulations (red) with a Boltzmann population distribution show that these three observed vibrational levels of NO products have cold rotational temperatures of ~ 60 K. The vibrational temperature of NO products from 1-methyl-2,4,5-trinitroimidazole is estimated to be ~ 1350 K.

judge which one of them is energetically more favorable for multinitroimidazoles.

The energy barriers for NO_2 elimination and nitro–nitrite isomerization of multinitroimidazoles (1,4-dinitroimidazole, 2,4-dinitroimidazole, 1-methyl-2,4-dinitroimidazole, and 1-methyl-2,4,5-trinitroimidazole) on their electronic ground states from the Franck–Condon equilibrium geometry are reported in Table 2. NO_2 elimination and nitro–nitrite isomerization of all NO_2 groups at the different positions on the imidazole aromatic ring have been calculated at the B3P86/6-311G(d,p) level of theory. Multinitroimidazoles (except for 1,4-dinitroimidazole) have comparable energy barriers of about 65 kcal/mol for both C– NO_2 homolysis and nitro–nitrite isomerization reaction channels. These energy barriers are not necessarily the only consideration for determination of a dominant reaction channel, however. Other dynamic and kinetic factors such as reaction enthalpy, reaction rate, etc. should also be taken into account to reveal the primary decomposition process, as has been reported⁸ for the gas phase thermal decomposition of HMX. Nonetheless, based on energy barriers alone, the NO_2 elimination and nitro–nitrite isomerization channels will compete with each other for the electronic ground state decomposition of these nitroimidazole model molecules from the Franck–Condon equilibrium point.

With regard to 1,4-dinitroimidazole, the energy barrier for NO_2 elimination from N1– NO_2 homolysis is 34.5 kcal/mol, which is much lower than that of the nitro–nitrite isomerization for N1– NO_2 (69.6 kcal/mol) or C4– NO_2 (61.0 kcal/mol). The weakest bond in the molecule will determine the decomposition reaction behavior, in this instance. Thus N– NO_2 homolysis is predicted to be the more favorable decomposition channel for the 1,4-dinitroimidazole remaining on the ground state PES.

To estimate the HONO elimination reaction channel, the energy barriers of HONO elimination for 2,4-dinitroimidazole have been calculated at the B3P86/6-311G(d,p) level as shown in Figure 7. This dissociation channel requires roughly 43.2

Table 2. Barriers (kcal/mol) for NO₂ Elimination and Nitro–Nitrite Isomerization for Different Compounds on Their Ground State Potential Energy Surfaces

| compds | methods | bond | NO ₂ elimination | nitro–nitrite isomerization | <i>h</i> _{50%} (cm) ^a |
|----------------------------------|-------------------------|--------------------------------|-----------------------------|-----------------------------|-------------------------------------------|
| 1,4-dinitroimidazole | B3P86/6-311G(d,p) | N1–NO ₂ | 34.5 | 69.6 | 55 |
| | | C4–NO ₂ | 70.0 | 61.0 | |
| 2,4-dinitroimidazole | B3P86/6-311G(d,p) | C2–NO ₂ | 69.1 | 61.3 | 105 |
| | | C4–NO ₂ | 70.1 | 64.6 | |
| 1-methyl-2,4-dinitroimidazole | B3P86/6-311G(d,p) | C2–NO ₂ | 67.4 | 58.2 | |
| 1-methyl-2,4,5-trinitroimidazole | B3P86/6-311G(d,p) | C4–NO ₂ | 70.5 | 64.7 | |
| | | C2–NO ₂ | 63.3 | 54.7 | |
| | | C4–NO ₂ | 61.7 | 52.3 | |
| HMX | | N–NO ₂ ^b | 38.1 | 46.3 | 32 |
| RDX | B-PW91/cc-pVDZ | N–NO ₂ ^c | 34.2 | | 28 |
| | ONIOM(MP2/6-31G(d):UFF) | N–NO ₂ ^d | 41.0 | 92.2 | |
| PETN | CAS(6,6)/6-31G(d) | O–NO ₂ ^e | 35 | 60 | 16 |
| | exptl | O–NO ₂ ^f | 36.1 | | |

^aReferences 4, 5, and 45. ^bReference 8. ^cReference 46. ^dReference 47. ^eReference 43. ^fReference 7.

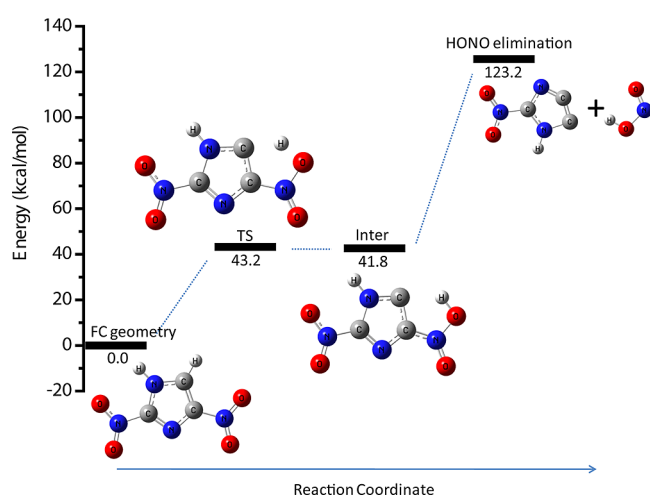


Figure 7. Potential energies and structures for HONO elimination from 2,4-dinitroimidazole. “TS” is the transition state for the H atom transferring from the C atom to the O atom. “Inter” is the intermediate for HONO elimination. “HONO elimination” is the final dissociated product. Surmounting the 123.2 kcal/mol energy barrier is required for HONO elimination compared to the Franck–Condon geometry of 2,4-dinitroimidazole.

kcal/mol activation energy to transfer the H atom from the C atom of the imidazole ring to the O atom of the NO₂ moiety. After forming the HONO elimination intermediate, 81.4 kcal/mol activation energy is required to break the C–N bond and produce HONO. The total energy barrier is about 123.2 kcal/mol, which is much higher than the barriers of NO₂ elimination and nitro–nitrite isomerization. Thus the HONO elimination reaction channel is excluded for the decomposition process of multinitroimidazoles.

B. Decomposition Following Excitation to Electronic Excited States. TD-DFT calculations of the electronic excitation energies of nitrobenzene at the LC- ω PBE/aug-cc-pVDZ and LC-BLYP/aug-cc-pVDZ levels have been performed by Jason et al.³⁷ The calculated results are in good agreement with the experimental results. Thus the vertical excitation energies for 1,4-dinitroimidazole and 2,4-dinitroimidazole have been explored at the LC- ω PBE/aug-cc-pVDZ³⁸ and LC-BLYP/aug-cc-pVDZ³⁹ level: the results of this calculation are listed in

Table 3. Comparison of the excitation energies (5.49 eV at 226 nm, 5.25 eV at 236 nm, and 5.00 eV at 248 nm) used in this

Table 3. Electronic Excitation Energies (eV) of 1,4-Dinitroimidazole and 2,4-Dinitroimidazole

| electronic excited states | 1,4-dinitroimidazole | | 2,4-dinitroimidazole | |
|---------------------------|----------------------------------|-------------------------|----------------------------------|-------------------------|
| | TD-LC- ω PBE ^a | TD-LC-BLYP ^a | TD-LC- ω PBE ^a | TD-LC-BLYP ^a |
| S ₁ | 3.82 | 3.87 | 3.81 | 3.85 |
| S ₂ | 4.28 | 4.34 | 3.85 | 3.91 |
| S ₃ | 4.38 | 4.42 | 4.30 | 4.37 |
| S ₄ | 4.93 | 5.02 | 4.34 | 4.40 |
| S ₅ | 5.00 | 5.06 | 5.07 | 5.14 |
| S ₆ | 5.71 | 5.81 | 5.54 | 5.60 |
| S ₇ | 6.11 | 6.18 | 5.92 | 6.09 |
| S ₈ | 6.21 | 6.25 | 6.16 | 6.13 |

^aaug-cc-pVDZ basis set.

work with the calculated vertical excitation energies suggests that these nitroimidazole energetic molecules may be excited at least to their S₅ electronic excited states. Due to the large number of nonbonding electrons in these nitroaromatic compounds and the high excited states involved in the reaction, entire potential energy surfaces have not been explored by the CASSCF method, as we have done for other energetic systems.²⁴

The optimized structures (S₀ equilibrium or Franck–Condon position) for 1,4-dinitroimidazole and 2,4-dinitroimidazole on the ground state surface employing a CASSCF active space of (16, 12) are shown in panels a and d of Figure 8. These two optimized geometries belong to the C_s point group and the nitro groups are in the plane of the imidazole ring. A small active space CASSCF (8, 6), in which all chosen orbitals are mostly located on one nitro group as shown in Figure 2, is used to search for conical intersections,^{48–51} even though we cannot explore whole PESs within this approximation.

Figure 8 shows the geometries at the conical intersections between the ground state (S₀) and the first excited state (S₁) for 1,4-dinitroimidazole and 2,4-dinitroimidazole. Two conical intersections have been found for each dinitroimidazole. Figure 8b is the geometry of the conical intersection between S₀ and S₁ for 1,4-dinitroimidazole considering only the NO₂ group

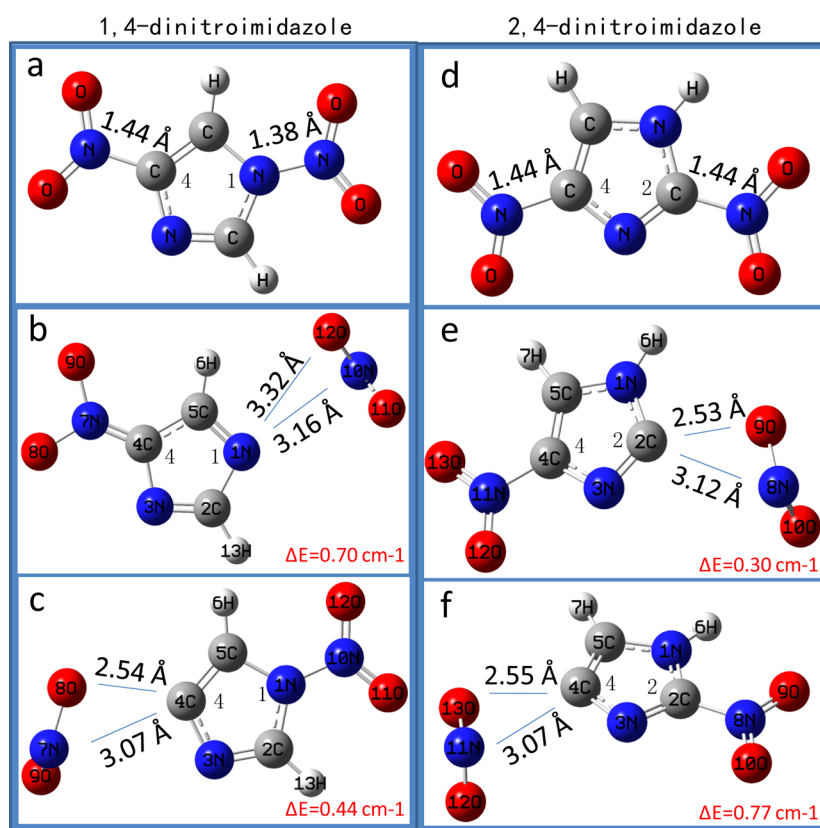


Figure 8. (a and d) The minimum energy geometries of 1,4-dinitroimidazole and 2,4-dinitroimidazole on the ground state optimized at the CASSCF(16, 12)/6-31G(d) level. (b and c) S_1/S_0 conical intersection geometries for 1,4-dinitroimidazole calculated at the CASSCF(8, 6)/6-31G(d) level. (e and f) S_1/S_0 conical intersection geometries for 2,4-dinitroimidazole calculated at the CASSCF(8, 6)/6-31G(d) level. ΔE is the energy gap between S_1 and S_0 at the conical intersection point.

located on the N1 atom of the imidazole ring. Figure 8c is the geometry of the other conical intersection between S_0 and S_1 of 1,4-dinitroimidazole considering only the NO_2 group located on the C4 atom of the imidazole ring. The energy gaps between S_0 and S_1 at the conical intersections are 0.70 and 0.44 cm^{-1} , respectively. Figure 8e shows the geometry at the conical intersection between S_0 and S_1 of 2,4-dinitroimidazole considering only the NO_2 group located on the C2 atom of the imidazole ring. Figure 8f is the geometry of the other conical intersection between S_0 and S_1 of 2,4-dinitroimidazole considering only the NO_2 group located on the C4 atom of the imidazole ring. The energy gaps between S_0 and S_1 for these conical intersections are 0.30 and 0.77 cm^{-1} , respectively. The small adiabatic energy gaps between S_0 and S_1 suggest that the S_1 and S_0 surfaces are strongly nonadiabatically coupled at all these conical intersection points. This strong coupling implies that excited nitroimidazole energetic molecules undergo (nonadiabatic) transitions from the excited electronic state to the ground state through the conical intersection $(S_1/S_0)_{\text{CI}}$. Two conical intersections $(S_1/S_0)_{\text{CI}}$ found for nitroimidazole energetic molecules may imply that the more nitro groups on the imidazole ring, the greater the probability for conical intersections between the various PESs.

VI. DISCUSSION

A. Decomposition Mechanism Following Excitation to Electronic Excited States. Based on our previous research on energetic materials,^{43,44,47,51,52} conical intersections play a crucial role in the decomposition process of electronically

excited energetic molecules; most excited energetic molecules descend to the ground state through a series of conical intersections, and generate, for an NO_2 containing molecule, an NO molecule following a nitro–nitrite isomerization on the ground state surface. Previous study²⁴ also reveals that conical intersections $(S_2/S_1)_{\text{CI}}$ and $(S_1/S_0)_{\text{CI}}$ have been found for mononitroimidazoles (model), which mostly descend to the first electronic excited state through conical intersections $(S_2/S_1)_{\text{CI}}$ and then generate an NO molecule following a nitro–nitrite isomerization. Multinitroimidazoles (energetic) of course have more complex PESs compared to mononitroimidazoles due to additional nitro groups on the aromatic ring. Thus the nonadiabatic vibronic coupling between each PES of multinitroimidazoles should experience a significant increase over that found for the mononitroimidazoles. Quenneville et al.³⁷ have calculated the excited state PESs of TNT using time-dependent density functional theory and multiconfigurational ab initio methods, and also found multiple conical intersections $(S_1/S_0)_{\text{CI}}$. They consider that for TNT the $S_1 \rightarrow S_0$ de-excitation pathways are similar to those for nitrobenzene, and access to the nonadiabatic region is controlled by motion of a single NO_2 group. Thus the probability of relaxation from S_1 to S_0 through nonadiabatic coupling (conical intersection) increases with the number of NO_2 groups for aromatic energetic molecules, such as multinitroimidazoles as well.

As shown in Figures 3–6, the experimental results indicate that the NO product from multinitroimidazoles has an excited vibrational distribution and the vibrational temperature is as high as 1600 K. The high vibrational excitation can be obtained

only when the molecule stores significant electronic excitation energy that can be used to excite vibrational degrees of freedom after it descends back to the ground state surface.

Figure 9 represents the final transition states for NO elimination from nitro–nitrite isomerization of 1,4-dinitroimidazole

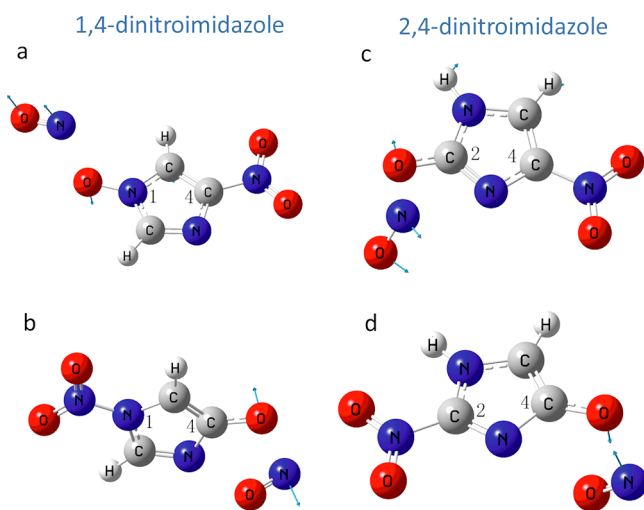


Figure 9. Transition states for NO elimination from nitro–nitrite isomerization on the electronic ground state calculated at the CASSCF(8, 6)/6-31G(d) level. The arrows on the structures of the transition states show the reaction coordinate of the imaginary frequency. (a) The transition state for NO elimination for the NO₂ moiety on the N1 atom of 1,4-dinitroimidazole. (b) The transition state for NO elimination for the NO₂ moiety on the C4 atom of 1,4-dinitroimidazole. (c) The transition state for NO elimination for the NO₂ moiety on the C2 atom of 2,4-dinitroimidazole. (d) The transition state for NO elimination for the NO₂ moiety on the C4 atom of 2,4-dinitroimidazole.

dazole and 2,4-dinitroimidazole on the electronic ground state calculated at the CASSCF(8, 6)/6-31G(d) level. The imaginary frequency mode of vibration associated with the relevant transition state on the ground electronic state surface does not generate a resultant torque on the NO moiety during dissociation of the parent molecule: this reaction coordinate generates an NO product with a cold rotational distribution. This conclusion is in a good agreement with our experimental results.

Kimmel et al.⁵³ studied the isolated energetic molecule 1,1-diamino-2,2-dinitroethylene (FOX-7) by means of density functional theory. They also find that the nitro–nitrite rearrangement followed by CO–NO bond homolysis is an important decomposition channel, especially, for excitation of the neutral FOX-7 molecule.

As discussed above, despite the inability to calculate entire PESs for multinitroimidazole molecules, we conclude that excited multinitroimidazoles descend to the ground state through a series of conical intersections and dissociate on the ground state PES after nitro–nitrite isomerization to produce an NO initial decomposition product. This $S_n \rightarrow \dots \rightarrow S_0$ pathway through a series of CIs leaves the molecule on a new part of the S_0 PES not necessary near the FC equilibrium point.

B. Relationship between Impact Sensitivities and Bond Dissociation Energies. Impact sensitivity is an important performance parameter for energetic materials. Calculation and prediction of the impact sensitivity for energetic materials can aid in the design of new energetic

materials with better stability and impact/shock insensitivity for multiple applications. As is well-known, the bond strength of the weakest bond for an energetic molecule is of considerable importance, since the rupture of this linkage can be a key factor in many decomposition processes. Usually the bond R–NO₂ (R = C, N, or O) is the weakest one in an energetic molecule and rupture of that bond can be the first step in the decomposition process from the S_0 equilibrium geometry. Thus, the stability and impact/shock sensitivity of energetic materials have been related to the strengths of the R–NO₂ bonds, which have been studied by several groups.^{4–6,22,23,54}

In this discussion, the barriers to dissociation and the bond dissociation energies for the R–NO₂ bond are numerically equivalent based on our calculated results. Thus the barriers for NO₂ elimination shown in Table 2 are treated as the bond dissociation energies for the R–NO₂ bond in the following discussion. As shown in Table 2, even though calculational methods for these energetic materials are different, the basic trend still can be obtained that the C–NO₂ bond, which requires an average of 65 kcal/mol of energy to break, is much stronger than the N–NO₂ and O–NO₂ bonds, which require only 35–45 kcal/mol to rupture. In other words, the C–NO₂ energetic materials are more thermally stable and less impact sensitive than N–NO₂ and O–NO₂ energetic materials. The impact sensitivity values $h_{50\%}$ (the height from which a given weight falling upon the compound gives a 50% probability of initiating an explosion) obtained by other research groups^{4,5,45} for 1,4-dinitroimidazole, 2,4-dinitroimidazole, HMX, RDX, and PETN are 55, 105, 32, 28, and 16 cm, respectively. Our prediction that multinitroimidazoles (C–NO₂) are more stable than HMX, RDX, and PETN (N–NO₂, O–NO₂) is in good agreement with these results. The imidazole aromatic ring also can help improve the stability of energetic materials, comparing 1,4-dinitroimidazole (55 cm), HMX (32 cm), and RDX (28 cm), which all have a weak N–NO₂ bond. The impact sensitivity value $h_{50\%}$ for TNT (C–NO₂) is 160 cm,⁴⁵ which also demonstrates that an aromatic ring can improve the stability of energetic materials. These correlations and comparisons suggest that energetic materials with a C–NO₂ moiety are more thermally stable and impact/shock insensitive than are those with N–NO₂ and O–NO₂ moieties; an aromatic ring can also improve stability of energetic materials. Aromatic moieties should play an important role in the future synthesis of new energetic materials.

VII. CONCLUSIONS

The initial steps in release of the stored chemical energy for four multinitroimidazole energetic molecules (1,4-dinitroimidazole, 2,4-dinitroimidazole, 1-methyl-2,4-dinitroimidazole, and 1-methyl-2,4,5-trinitroimidazole) have been studied experimentally and theoretically. These multinitroimidazoles generate NO as the dominant initial decomposition product, with vibrationally hot (1300–1600 K) and rotationally cold (10–60 K) internal energy distributions, following excitation at the nanosecond laser wavelengths (248, 236, 226 nm). These excitation energies correspond to three vibronic transitions, $A^2\Sigma^+ (v'=0) \leftarrow X^2\Pi (v''=0,1,2)$ of the NO molecule. The observed decomposition behavior is independent of excitation wavelength. These results are consistent with our previous research on energetic materials.^{43,44,47,51,52}

S_1/S_0 conical intersections have been found for 1,4-dinitroimidazole and 2,4-dinitroimidazole, and small energy gaps between S_1 and S_0 at conical intersection points imply

strong nonadiabatic coupling of the respective adiabatic PESs. The final reaction coordinate, the imaginary frequency for the transition states for NO elimination from nitro–nitrite isomerization for 1,4-dinitroimidazole and 2,4-dinitroimidazole, does not generate a large component of torque on the eliminated NO; the product NO is thereby expected to be rotationally cold, in agreement with experimental results. Although excited PESs have not been explored for this system, we can conclude that the possible reaction mechanism for the decomposition of multinitroimidazoles after electronic excitation is the following: electronically excited multinitroimidazoles descend to their ground electronic state through a series of conical intersections, dissociate on the ground state PES subsequent to nitro–nitrite isomerization, and produce vibrationally hot and rotationally cold NO products.

Thermal decomposition (electronic ground state decomposition from the Franck–Condon equilibrium point) of multinitroimidazoles exhibits a complex reaction process. For most multinitroimidazoles containing only the C–NO₂ moiety, NO₂ elimination and NO elimination following nitro–nitrite isomerization are competitive channels on the ground electronic state PES from the S₀ equilibrium geometry. Due to the relatively large difference between the energy barriers for C–NO₂ and N–NO₂ elimination, the above result is different from that found for HMX and RDX, for which NO₂ elimination can be the main decomposition channel on the ground state PES starting at the S₀ equilibrium geometry.

The relative strength of the weakest C–NO₂, N–NO₂, and O–NO₂ bonds in different energetic materials can often be related to the stability and impact/shock sensitivity of the energetic material. Energetic materials of the C–NO₂ type usually are more thermally stable and less impact/shock sensitive than those with N–NO₂ and O–NO₂ bonds for NO₂ containing energetic materials. Aromatic rings, such as benzene and imidazole, can also improve the stability of the energetic material by enhancing the R–NO₂ (R = C, N, O) bond strength.

Further study of electronically excited nitroimidazole energetic materials is still needed to check the prediction for the de-excitation pathway. Other multireference correlation methods (beside CASSCF) may be needed to explore the whole PESs, even though such calculations are expected to be expensive.

AUTHOR INFORMATION

Corresponding Author

*Tel: 1-970-491-6347. E-mail: erb@lamar.colostate.edu.

Notes

The authors declare no competing financial interest.

ACKNOWLEDGMENTS

This study is supported by a grant from the U.S. Army Research Office (ARO, FA9550-10-1-0454) and in part by the U.S. National Science Foundation (NSF) through the XSEDE supercomputer resources provided by SDSC under grant no. TG-CHE110083. We thank Dr. Rao Surapaneni and Mr. Reddy Damavarapu (ARL, Picatinny Arsenal, NJ) for supplying the samples used in this research.

REFERENCES

(1) Butler, L. J.; Krajinovich, D.; Lee, Y. T.; Ondrey, G. S.; Bersohn, R. The Photodissociation of Nitromethane at 193 nm. *J. Chem. Phys.* **1983**, *79*, 1708–1722.

(2) Shigeto, S.; Pang, Y.; Fang, Y.; Dlott, D. D. Vibrational Relaxation of Normal and Deuterated Liquid Nitromethane. *J. Phys. Chem. B* **2008**, *112*, 232–241.

(3) Surber, E.; Lozano, A.; Lagutchev, A.; Kim, H.; Dlott, D. D. Surface Nonlinear Vibrational Spectroscopy of Energetic Materials: HMX. *J. Phys. Chem. C* **2007**, *111*, 2235–2241.

(4) Rice, B. M.; Sahu, S.; Owens, F. J. Density Functional Calculations of Bond Dissociation Energies for NO₂ Scission in Some Nitroaromatic Molecules. *J. Mol. Struct.: THEOCHEM* **2002**, *583*, 69–72.

(5) Rice, B. M.; Hare, J. J. A Quantum Mechanical Investigation of the Relation between Impact Sensitivity and the Charge Distribution in Energetic Molecules. *J. Phys. Chem. A* **2002**, *106*, 1770–1783.

(6) Politzer, P.; Murray, J. S. C–NO₂ Dissociation Energies and Surface Electrostatic Potential Maxima in Relation to the Impact Sensitivities of Some Nitroheterocyclic Molecules. *Mol. Phys.* **1995**, *86*, 251–255.

(7) Aluker, E. D.; Krechetov, A. G.; Mitrofanov, A. Y.; Nurmukhametov, D. R.; Kuklja, M. M. Laser Initiation of Energetic Materials: Selective Photoinitiation Regime in Pentaerythritol Tetranitrate. *J. Phys. Chem. C* **2011**, *115*, 6893–6901.

(8) Sharia, O.; Kuklja, M. M. Ab Initio Kinetics of Gas Phase Decomposition Reactions. *J. Phys. Chem. A* **2010**, *114*, 12656–12661.

(9) Manaa, M. R.; Reed, E. J.; Fried, L. E.; Goldman, N. Nitrogen-Rich Heterocycles as Reactivity Retardants in Shocked Insensitive Explosives. *J. Am. Chem. Soc.* **2009**, *131*, 5483–5487.

(10) Manaa, M. R.; Schmidt, R. D.; Overturf, G. E.; Watkins, B. E.; Fried, L. E.; Kolb, J. R. Towards Unraveling the Photochemistry of TATB. *Thermochim. Acta* **2002**, *384*, 85–90.

(11) Reed, E. J. Electron-Ion Coupling in Shocked Energetic Materials. *J. Phys. Chem. C* **2012**, *116*, 2205–2211.

(12) Badgular, D. M.; Talawar, M. B.; Asthana, S. N.; Mahulikar, P. P. Advances in Science and Technology of Modern Energetic Materials: An Overview. *J. Hazard. Mater.* **2008**, *151*, 289–305.

(13) Agrawal, J. P.; Hodgson, R. D. *Organic Chemistry of Explosives*; John Wiley & Sons: Hoboken, NJ, 2007.

(14) Pagoria, P. F.; Lee, G. S.; Mitchell, A. R.; Schmidt, R. D. A Review of Energetic Materials Synthesis. *Thermochim. Acta* **2002**, *384*, 187–204.

(15) Lee, J. C.; Laydon, J. T.; McDonnell, P. C.; Gallagher, T. F.; Kumar, S.; Green, D.; McNulty, D.; Blumenthal, M. J.; Heys, J. R.; Landvatter, S. W.; et al. A Protein-kinase Involved in the Regulation of Inflammatory Cytokine Biosynthesis. *Nature* **1994**, *372*, 739–746.

(16) Kuhn, N.; Kratz, T. Synthesis of Imidazole-2-Ylidenes by Reduction of Imidazole-2(3H)-Thiones. *Synthesis* **1993**, *1993*, 561–562.

(17) Cho, S. G.; Cheun, Y. G.; Park, B. S. A Computational Study of Imidazole, 4-Nitroimidazole, 5-Nitroimidazole and 4,5-Dinitroimidazole. *J. Mol. Struct.: THEOCHEM* **1998**, *432*, 41–53.

(18) Cho, J. R.; Kim, K. J.; Cho, S. G.; Kim, J. K. Synthesis and Characterization of 1-methyl-2,4,5-trinitroimidazole (MTNI). *J. Heterocycl. Chem.* **2002**, *39*, 141–147.

(19) Gutowski, K. E.; Rogers, R. D.; Dixon, D. A. Accurate Thermochemical Properties for Energetic Materials Applications. I. Heats of Formation of Nitrogen-Containing Heterocycles and Energetic Precursor Molecules from Electronic Structure Theory. *J. Phys. Chem. A* **2006**, *110*, 11890–11897.

(20) Gutowski, K. E.; Rogers, R. D.; Dixon, D. A. Accurate Thermochemical Properties for Energetic Materials Applications. II. Heats of Formation of Imidazolium-, 1,2,4-Triazolium-, and Tetrazolium-Based Energetic Salts from Isodesmic and Lattice Energy Calculations. *J. Phys. Chem. B* **2007**, *111*, 4788–4800.

(21) Jadhav, H. S.; Talawar, M. B.; Sivabalan, R.; Dhavale, D. D.; Asthana, S. N.; Krishnamurthy, V. N. Synthesis, Characterization and Thermolysis Studies on New Derivatives of 2,4,5-Trinitroimidazoles: Potential Insensitive High Energy Materials. *J. Hazard. Mater.* **2007**, *143*, 192–197.

- (22) Li, X. H.; Zhang, R. Z.; Zhang, X. Z. Computational Study of Imidazole Derivative as High Energetic Materials. *J. Hazard. Mater.* **2010**, *183*, 622–631.
- (23) Su, X. F.; Cheng, X. L.; Meng, C. M.; Yuan, X. L. Quantum Chemical Study on Nitroimidazole, Polynitroimidazole and their Methyl Derivatives. *J. Hazard. Mater.* **2009**, *161*, 551–558.
- (24) Yu, Z.; Bernstein, E. R. Experimental and Theoretical Studies of the Decomposition of New Imidazole Based Energetic Materials: Model Systems. *J. Chem. Phys.* **2012**, *137*, 114303.
- (25) Bhattacharya, A.; Guo, Y. Q.; Bernstein, E. R. Experimental and Theoretical Exploration of the Initial Steps in the Decomposition of a Model Nitramine Energetic Material: Dimethylnitramine. *J. Phys. Chem. A* **2009**, *113*, 811–823.
- (26) (a) Bhattacharya, A.; Guo, Y.; Bernstein, E. R. Nonadiabatic Reaction of Energetic Molecules. *Acc. Chem. Res.* **2010**, *43*, 1476–1485. (b) Shaw, R. W.; Brill, T. B.; Thompson, D. L. *Overviews of recent research on energetic materials*; World Scientific: Hackensack, NJ, 2005; Chapters 6, 8, 9, and 11. (3) For a general reference to “triboluminescence” see: <http://en.wikipedia.org/wiki/Triboluminescence>.
- (27) Im, H. S.; Bernstein, E. R. On the Initial Steps in the Decomposition of Energetic Materials from Excited Electronic States. *J. Chem. Phys.* **2000**, *113*, 7911–7918.
- (28) Guo, Y. Q.; Greenfield, M.; Bernstein, E. R. Decomposition of Nitramine Energetic Materials in Excited Electronic States: RDX and HMX. *J. Chem. Phys.* **2005**, *122*, 244310.
- (29) Frisch, M. J.; Trucks, G. W.; Schlegel, H. B.; Scuseria, G. E.; Robb, M. A.; Cheeseman, J. R.; Scalmani, G.; Barone, V.; Mennucci, B.; Petersson, G. A. et al. *Gaussian 09*, revision A.1; Gaussian, Inc.: Wallingford, CT, 2009.
- (30) Wu, C. J.; Fried, L. E. *11th Int. Detonation Symp.*, CO **1998**, 490–497.
- (31) Li, J.; Zhao, F.; Jing, F. An Ab Initio Study of Intermolecular Interactions of Nitromethane Dimer and Nitromethane Trimer. *J. Comput. Chem.* **2003**, *24*, 345–352.
- (32) Shao, J. X.; Cheng, X. L.; Yang, X. D. Density functional calculations of bond dissociation energies for removal of the nitrogen dioxide moiety in some nitroaromatic molecules. *J. Mol. Struct.* **2005**, *755*, 127–130.
- (33) Song, X.-S.; Cheng, X.-L.; Yang, X.-D.; He, B. Relationship between the Bond Dissociation Energies and Impact Sensitivities of Some Nitro-Explosives. *Propellants, Explosives, Pyrotechnics* **2006**, *31*, 306–310.
- (34) Li, J. An Evaluation of Nitro Derivatives of Cubane Using Ab Initio and Density Functional Theories. *Theor. Chem. Acc.* **2009**, *122*, 101–106.
- (35) Murray, J. S.; Concha, M. C.; Politzer, P. Links between Surface Electrostatic Potentials of Energetic Molecules, Impact Sensitivities and C-NO₂/N-NO₂ Bond Dissociation Energies. *Mol. Phys.* **2009**, *107*, 89–97.
- (36) Luo, Y. R. *Comprehensive handbook of chemical bond energies*; CRC Press: Boca Raton, FL, 2007.
- (37) Quenneville, J.; Greenfield, M.; Moore, D. S.; McGrane, S. D.; Scharff, R. J. Quantum Chemistry Studies of Electronically Excited Nitrobenzene, TNA, and TNT. *J. Phys. Chem. A* **2011**, *115*, 12286–12297.
- (38) Vydrov, O. A.; Heyd, J.; Krukau, A. V.; Scuseria, G. E. Importance of Short-Range Versus Long-Range Hartree-Fock Exchange for the Performance of Hybrid Density Functionals. *J. Chem. Phys.* **2006**, *125*, 074106.
- (39) Tawada, Y.; Tsuneda, T.; Yanagisawa, S.; Yanai, T.; Hirao, K. A Long-Range-Corrected Time-Dependent Density Functional Theory. *J. Chem. Phys.* **2004**, *120*, 8425–8433.
- (40) Palmer, I. J.; Ragazos, I. N.; Bernardi, F.; Olivucci, M.; Robb, M. A. An MC-SCF Study of the S₁ and S₂ Photochemical Reactions of Benzene. *J. Am. Chem. Soc.* **1993**, *115*, 673–682.
- (41) Simpson, C. J. S. M.; Griffiths, P. T.; Wallaart, H. L.; Towrie, M. Photodissociation of Alkyl Nitrites Adsorbed on an MgF₂ Surface. Rotational and Translational Energy Distributions of Product NO(v, J) molecules. *Chem. Phys. Lett.* **1996**, *263*, 19–24.
- (42) Herzberg, G. *Molecular Spectra and Molecular Structure: Spectra of Diatomic Molecules*; Van Nostrand Reinhold Co.: New York, NY, 1950.
- (43) Yu, Z. J.; Bernstein, E. R. Decomposition of Pentaerythritol Tetranitrate C(CH₂ONO₂)₄ following Electronic Excitation. *J. Chem. Phys.* **2011**, *135*, 154305.
- (44) Guo, Y. Q.; Greenfield, M.; Bhattacharya, A.; Bernstein, E. R. On the Excited Electronic State Dissociation of Nitramine Energetic Materials and Model Systems. *J. Chem. Phys.* **2007**, *127*, 154301.
- (45) Storm, C. B.; Stine, J. R.; Kramer, J. F. *Chemistry and Physics of Energetic Materials*; Kluwer Academic Publishers: Dordrecht, The Netherlands, 1990; pp 605–639.
- (46) Wu, C. J.; Fried, L. E. Ab Initio Study of RDX Decomposition Mechanisms. *J. Phys. Chem. A* **1997**, *101*, 8675–8679.
- (47) Bhattacharya, A.; Bernstein, E. R. Nonadiabatic Decomposition of Gas-Phase RDX through Conical Intersections: An ONIOM-CASSCF Study. *J. Phys. Chem. A* **2011**, *115*, 4135–4147.
- (48) Asturiol, D.; Lasorne, B.; Worth, G. A.; Robb, M. A.; Blancafort, L. Exploring the Sloped-to-Peaked S₂/S₁ Seam of Intersection of Thymine with Electronic Structure and Direct Quantum Dynamics Calculations. *Phys. Chem. Chem. Phys.* **2010**, *12*, 4949–4958.
- (49) Peláez, D.; Arenas, J. F.; Otero, J. C.; Soto, J. Dependence of N-Nitrosodimethylamine Photodecomposition on the Irradiation Wavelength: Excitation to the S₂ State as a Doorway to the Dimethylamine Radical Ground-State Chemistry. *J. Org. Chem.* **2007**, *72*, 4741–4749.
- (50) Soto, J.; Arenas, J. F.; Otero, J. C.; Peláez, D. Effect of an S₁/S₀ Conical Intersection on the Chemistry of Nitramide in Its Ground State. A Comparative CASPT2 Study of the Nitro-Nitrite Isomerization Reactions in Nitramide and Nitromethane. *J. Phys. Chem. A* **2006**, *110*, 8221–8226.
- (51) Guo, Y. Q.; Bhattacharya, A.; Bernstein, E. R. Excited Electronic State Decomposition of Furazan Based Energetic Materials: 3,3'-Diamino-4,4'-Azoxylfuran and its Model Systems, Diaminofurazan and Furazan. *J. Chem. Phys.* **2008**, *128*, 034303.
- (52) Bhattacharya, A.; Guo, Y. Q.; Bernstein, E. R. Unimolecular Decomposition of Tetrazine-N-oxide Based High Nitrogen Content Energetic Materials from Excited Electronic States. *J. Chem. Phys.* **2009**, *131*, 194304.
- (53) Kimmel, A. V.; Sushko, P. V.; Shluger, A. L.; Kuklja, M. M. Effect of Charged and Excited States on the Decomposition of 1,1-Diamino-2,2-Dinitroethylene Molecules. *J. Chem. Phys.* **2007**, *126*, 234711.
- (54) Li, J. Relationships for the Impact Sensitivities of Energetic C-Nitro Compounds Based on Bond Dissociation Energy. *J. Phys. Chem. B* **2010**, *114*, 2198–2202.